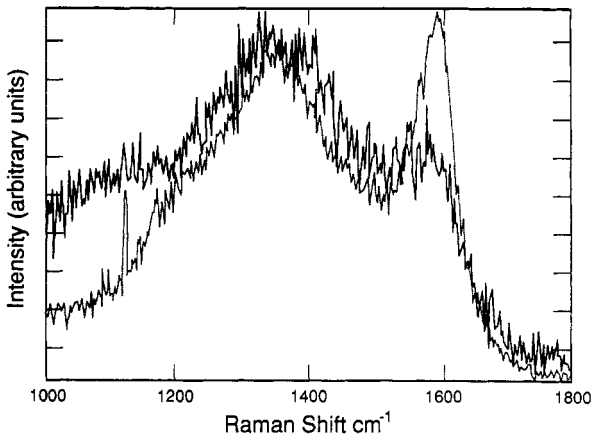

Figure 6. Raman spectra of benzene-(dotted line) and triphenylene- (solid line) derived graphites prepared at 800 °C.

mobile electrons in the more ordered structure. The dependence of line width on temperature for both 800 °C products (Table II) shows a very small activation energy. The spin concentration of B (800 °C) is twice that of TP (800 °C) and probably indicates the greater number of reactive sites per ring in benzene.

A comparison of the Raman spectra of TP and B flakes at 800 °C is given in Figure 6. The ratios of the intensity of the order peak to that of disorder peak are quite different in the two materials, offering additional evidence of the different degree of orientation of the as-deposited carbons. At an HTT of 2600 °C, the disorder peak disappears in all of these samples to yield the conventional graphite Raman spectrum.[23]

Conclusions

The structure of the aromatic hydrocarbon precursor strongly influences the nature of the graphitization process and hence the properties of the resulting graphite. The size and nature of aromatic radicals in the gas phase, their growth prior to nucleation, and the nucleation and growth on substrate are undoubtedly all involved in the process.[24] The larger size of the TP species results in a coarser microstructure with less order at low HTTs, complex morphologies of beaded structures, higher defect densities, and exfoliated regimes at higher HTTs. B-derived radicals appear to be ideal size nucleii, leading to high-quality graphite. Other small aromatics, such as bromobenzene, are also good starting materials for highly ordered graphites.

Acknowledgment. The assistance of Dr. G. Meyer and Dr. P. Heiney with the XRD and W. Shin with the Raman spectra is acknowledged, as well as helpful discussions with Dr. S. Jansen regarding interpretation of the ESR results. This work was supported by the National Science Foundation, Ceramics and Electronic Materials, Division of Materials Research, under Grant No. DMR87-03526. The XRD measurements of P. Heiney were performed using central facilities of the Laboratory for Research on the Structure of Matter, supported by the National Science Foundation Grant No. DMR MRL 88-19885.

Registry No. Benzene, 71-43-2; triphenylene, 217-59-4; graphite, 7782-42-5.

(23) Fischbach, D. B.; Couzi, M. *Carbon* **1986**, *24*, 365.
(24) Kaae, J. L. *Carbon* **1985**, *23*, 665.

Dielectric Response and Conductivity of Poly(propylene oxide) Sodium Polyiodide Complexes. Discussion of Charge Transfer by an Ion Relay Mechanism

Hans-Conrad zur Loye,[†,1] Bruce J. Heyen,[†] Henry O. Marcy,[‡] Donald C. DeGroot,[‡] Carl R. Kannewurf,[‡] and Duward F. Shriver*,[†]

Department of Chemistry and Department of Electrical Engineering and Computer Science, Northwestern University, Evanston, Illinois 60208

Received May 8, 1990

The addition of iodine to poly(propylene oxide), PPO, with or without NaI results in the formation of polyiodides as evidenced by a resonance Raman band at 170 cm^{-1}. The conductivities of these complexes, measured with ac and dc methods, show both ohmic and nonohmic responses characteristic of electronic and ionic conductors, respectively. The conductivity rises with both increasing iodine and salt concentrations. Low-temperature conductivity data showed a very small inflection in the vicinity of T_g for the host polymer, indicating that dynamics of the host polymer are only weakly coupled to the mechanism for conductivity in the polyiodide system. An ion relay along polyiodide chains is consistent with these observations. For comparison purposes, Raman spectra and conductivities were studied for structurally characterized metal compounds containing infinite I_3^- species. In these structures the conductivity is very low, and this is attributed to structural pinning of the polyiodides, which would block ion relay or carrier hopping charge transport.

Introduction

The study of new materials with variable stoichiometry and adjustable electronic properties has led to the discovery of a wealth of chemically interesting dielectric and electrical behavior. Recently, we have explored new polymer materials, polymer salt complexes containing polyiodides, which exhibit both ionic and electronic conductivity. Complexes of the composition $(PEO)_nNaI_x$, where PEO = poly(ethylene oxide), were first studied by

[†] Department of Chemistry.
[‡] Department of Electrical Engineering and Computer Science.

(1) Department of Chemistry, MIT, Cambridge, MA 02139.

0897-4756/90/2802-0603$02.50/0

Hardy and Shriver, and more recently, Lerner and coworkers studied polyiodide salt complexes of a polyphosphazene polymer.[2,3] The addition of I_2 to $(PEO)_nNaI$ results in a change of the electrical properties giving rise to an ohmic electrical response. The system reported here is $(PPO)_nNaI_x$, where PPO = atactic poly(propylene oxide). Atactic PPO is an amorphous polymer which eliminates the complexity of having both crystalline and amorphous regions in the same material, as encountered in PEO.

Until recently, most work with ionically conducting polymers has focused on semicrystalline PEO-based polymer salt complexes. In these materials the ionic conductivity is generally described by a free volume or VTF type theory,[4-6] which can be linked to the polymer segmental motion. Temperatures in excess of the glass transition temperature of the polymer salt complex are necessary for appreciable ionic conductivity. Additional information on the mechanism of ion conduction in polymeric materials is available.[6] Unlike the polyiodide-containing salt complexes, these materials do not exhibit electronic conductivity. The mechanisms proposed for electronic conductivity in polyacetylene and related conducting polymers do not appear to explain the electronic conductivity in the polyiodide-containing polymers.[7,8] In this paper, the electrical properties of polyiodide-containing polymers are characterized both above and below T_g. These data along with conductivity measurements on crystalline inorganic compounds containing $(I_3)_\infty$ chains provide insight into conduction mechanisms in polyiodides.

Experimental Section

Preparation of $(PPO)_nNaI_x$. Polymer salt complexes were prepared by dissolving poly(propylene oxide) and sodium iodide in a common solvent, methanol, followed by solvent removal under rough vacuum; the polymer salt complex was then dried under high vacuum and exposed to stoichiometric amounts of resublimed I_2 under an inert atmosphere at 60 °C to produce the polyiodide complex. The resulting polymer–polyiodide salt complexes are black. Polymer salt complexes, $(PPO)_nNaI_x$, were prepared with n = 4, 8, 16 and x = 1, 3, 5, 7, 9, and polymer–iodine complexes, PPO_nI_2, were prepared with n = 4, 8, 16, 32, 64. X-ray diffraction verified that these complexes are amorphous. All polymers and polymer salt complexes were handled under an inert atmosphere following preparation to prevent the introduction of moisture and oxygen.

Preparation and Characterization of Metal Complex Polyiodides. For comparison with the polymer polyiodides, the complexes $Cd(NH_3)_4I_6$[9] and $Ru(Me_2dtc)_3I_3$[10] (dtc = dithiocarbamato) were prepared by methods described in the references; the complexes $Ni(en)_2I_6$, $Cu(en)_2I_6$, and $Pd(en)_2I_6$ (en = ethylenediamine) were prepared by a method similar to the preparation of $Cd(NH_3)_4I_6$ starting with $Ni(en)_2SO_4$, $CuSO_4{\cdot}5H_2O$/ethylenediamine, and $Pd(en)_2I_2$,[11] respectively. Four-probe dc conductivities of single crystals of $Ni(en)_2I_6$ and $Ru(Me_2dtc)_3I_3$ were measured at room temperature with techniques previously described.[12] The dimensions of the crystals were approximately 0.5 mm × 0.1 mm × 0.05 mm for the ruthenium complex and 1 mm × 0.2 mm × 0.1 mm for the nickel complex. Electrodes were connected to the crystals with gold paste.

Physical Characterization of Polymer Systems. Electrical measurements were performed in an air-tight cell with a sample of approximately 1-mm thickness pressed between two $^1/_2$-in.-diameter disk electrodes. Stainless steel, tantalum, and gold-coated tantalum electrodes were used in the measurements. Ac impedance measurements were performed using a Hewlett-Packard 4192 LF impedance analyzer for high frequencies (5 Hz to 5 MHz) and a Solartron 1250 frequency response analyzer coupled to a Solartron 1286 electrochemical interface for low-frequency measurements (25 mHz to 10 kHz). Cyclic voltammetry was performed on the same cells between +20 and −20 mV at 1 mV/s on a BAS 100A electrochemical analyzer. Dc conductivity measurements were performed in the usual four-probe configuration using instrumentation and procedures described elsewhere.[12] Polymer samples were placed in a rectangular Teflon holder and sealed with a four-pin segment of an integrated circuit socket strip, which served as the measurement electrodes. The holder was mounted on a copper heat sink, and the conductivity measurements were carried out in a helium atmosphere to ensure temperature uniformity. For each data point, a total of 60 current and voltage determinations were averaged for each polarity of the applied current.

Resonance Raman spectra were recorded with Kr^+ (647.1 nm) or Ar^+ (514.5 nm) excitation and a Spex 1401 monochromator with photon-counting detection. Spectral resolution was normally 3 cm^{-1}. Samples were sealed under an inert atmosphere in 5-mm Pyrex tubes. All samples were probed with a 180° backscattering geometry,[13] and spinning was employed to reduce localized heating. Differential scanning calorimetry (DSC) was performed as previously described;[14] samples were loaded under an inert atmosphere in hermetically sealed aluminum pans.

Results and Discussion

Vibrational Spectra and Polyiodide Structure. The formation of polyiodides in the salt complexes can be described as a Lewis acid (I_2) base (I^- or I_{2n-1}^-) interaction.[15] Electron density is donated from the iodide anion into the antibonding orbitals of the I_2, which weakens and lengthens the I–I bond. This is reflected in the resonance Raman spectrum where the I–I stretching frequency shifts from its gas-phase position of 215 cm^{-1} to lower values in the polyiodide complexes. Polyiodides can also form via the disproportionation of nI_2 into ionic species. This disproportionation appears to occur to a small extent in molten I_2,[16] while in the presence of electron donors such as pyridine the disproportionation is extensive.[17] For instance, $[Py_2I^+][I_7^-]$ results when I_2 is dissolved in pyridine, and something similar may occur in the polymer complexes where the ether oxygens coordinate the cationic iodine species.

Polyiodides vary in shape from linear to zigzag, the specific conformation being strongly dependent on the counterion.[18] In all cases however, the pattern of bond lengths and angles can be described approximately as a combination of I^-, I_3^-, and I_2 units. In some instances I_3^- segments are spatially close enough to each other that they can be described as an $(I_3^-)_\infty$ chain; these chains have a repeating sequence of varying I–I bond lengths.[9,10,19]

(2) Hardy, L. C.; Shriver, D. F. *J. Am. Chem. Soc.* **1986**, *108*, 2887.
(3) Lerner, M. M.; Lyons, L. J.; Tonge, J. S.; Shriver, D. F. *Chem. Mater.* **1989**, *1*, 601.
(4) Vogel, H. *Phys. Z.* **1921**, *22*, 645. Fulcher, G. S. *J. Am. Ceram. Soc.* **1925**, *8*, 339. Tammann, G.; Hesse, W. *Z. Anorg. Allg. Chem.* **1926**, *156*, 217.
(5) Cohen, M. H.; Turnbull, D. *J. Chem. Phys.* **1959**, *31*, 1164. Grest, G. S.; Cohen, M. H. *Phys. Rev. B* **1980**, *21*, 4113.
(6) Ratner, M. A.; Shriver, D. F. *Chem. Rev.* **1988**, *88*, 109.
(7) *Polymers in Electronics*; Davidson, T., Ed.; American Chemical Society: Washington, D. C., 1984.
(8) Marks, T. J. *Science* **1985**, *227*, 881.
(9) Tebbe, K.-F.; Plewa, M. *Z. Anorg. Allg. Chem.* **1982**, *489*, 111.
(10) (a) Duffy, D. J.; Pignolet, L. H. *Inorg. Chem.* **1974**, *13*, 2045. (b) Mattson, B. M.; Pignolet, L. H. *Inorg. Chem.* **1977**, *16*, 488.
(11) Watt, G. W.; Layton, R. J. *J. Am. Chem. Soc.* **1960**, *82*, 4465.
(12) Lyding, J. W.; Marcy, H. O.; Marks, T. J.; Kannewurf, C. R. *IEEE Trans. Instrum. Meas.* **1988**, *37*, 76.
(13) Shriver, D. F.; Dunn, J. B. R. *Appl. Spectrosc.* **1974**, *28*, 319.
(14) Stainer, M.; Whitmore, D. H.; Shriver, D. F. *J. Electrochem. Soc.* **1984**, *131*, 784. Hardy, L. C.; Shriver, D. F. *J. Am. Chem. Soc.* **1985**, *107*, 3823.
(15) Marks, T. J. *Ann. N.Y. Acad. Sci.* **1978**, *313*, 594.
(16) Bearcroft, D. J.; Nachtrieb, N. H. *J. Phys. Chem.* **1967**, *71*, 316.
(17) Hassel, O.; Hope, H. *Acta. Chem. Scand.* **1961**, *15*, 407.
(18) Tebbe, K.-F. In *Homoatomic Rings, Chains, and Macromolecules of Main-Group Elements*; Rheingold, A. L., Ed.; Elsevier: New York, 1977; pp 551–606.

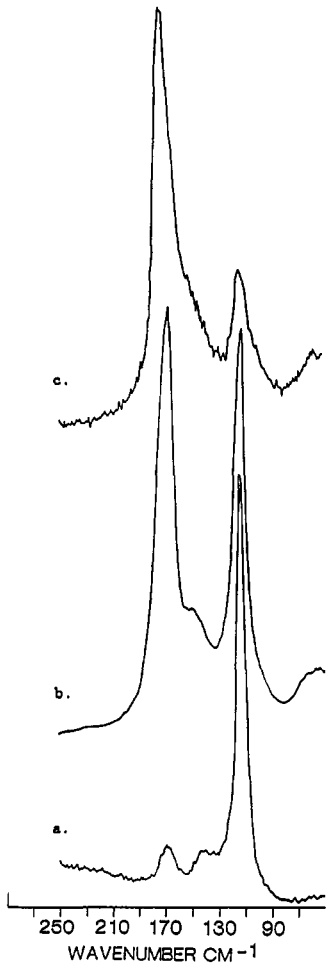

Figure 1. Resonance Raman spectra of (a) $(PPO)_{16}NaI_3$, (b) $(PPO)_8NaI_3$, and (c) $(PPO)_4NaI_3$. Peaks due to I_3^- at 114 cm^{-1} and higher polyiodides I_{2n-1}^- at 171 cm^{-1}. ν_0 = 647.1 nm.

Resonance Raman spectroscopy has been used by a number of investigators to characterize compounds containing polyiodides and to identify the different polyiodide species present in such materials.[20] Figure 1 shows the resonance Raman spectra of $(PPO)_4NaI_3$, $(PPO)_8NaI_3$, and $(PPO)_{16}NaI_3$. In all three spectra there are two Raman bands of varying intensity, one near 114 cm^{-1} and one at 171 cm^{-1}. Peaks in the 110–120-cm^{-1} range are assigned to the symmetric stretching mode of an I_3^- species, while peaks near 170 cm^{-1} are assigned to higher polyiodides.[15] The relative peak intensities change as the salt concentration in the polymer is increased (decreasing "n"). For a complex with low salt concentration, as in $(PPO)_{16}NaI_3$, an intense peak at 114 cm^{-1} is observed, while the peak at 170 cm^{-1} is weak. This suggests that for low salt concentrations most of the iodine is present as isolated I_3^-. When the NaI_3 concentration is increased, the peak at 170 cm^{-1} grows in intensity at the expense of the 114-cm^{-1} peak, shown in Figure 1b,c. In Figure 1c the 170-cm^{-1} peak now dominates the spectrum, which indicates that the individual triiodide ions have associated into longer chains. The 114-cm^{-1} band persists in all PPO polyiodide complexes studied here; by contrast this band disappears in PEO polyiodide complexes. Apparently the association is less complete in PPO. In all cases resonances corresponding to free I_2 (solid, 181, 191 cm^{-1}; in diethyl ether, 206 cm^{-1}; gas, 215 cm^{-1}) are not observed.

Table I. Raman Spectral Data (cm^{-1}) for PPO_nNaI_x (ν_0 = 647.1)

x	$(PPO)_4NaI_x$	$(PPO)_8NaI_x$	$(PPO)_{16}Na_x$
3	113, 169	116, 172, 140 (sh)	114, 170, 140 (sh)
5	112, 172	111, 171, 140 (sh)	111, 168, 140 (sh)
7	112, 174	110, 174	111, 169
9	113, 174	113, 175	111, 170

Table II. Summary of Raman Peak Widths (cm^{-1}) at Half-Height of the 170-cm^{-1} Band for PPO_nNaI_x (ν_0 = 647.1)

x	$(PPO)_4NaI_x$	$(PPO)_8NaI_x$	$(PPO)_{16}NaI_x$
3	17.2	15.2	11.0
5	27.2	22.5	17.6
7	32.0	27.5	20.0
9	34.0	30.0	25.6

Table III. Raman Data for Various Polyiodide-Containing Materials

compound	I–I dist, Å	Raman peaks, cm^{-1}	chain type
$Cd(NH_3)_4I_6$[11]	3.378, 2.745	171 (s)	linear
$Ru(dtc)_3I_3$[12b]	3.379, 2.830	155 (s), 170 (sh)	zigzag
$Ni(en)_2I_6$[19]	3.358, 3.326	112 (w), 154 (s), 210 (w, br)	zigzag
$Pd(en)_2I_6$[19]	3.598, 2.84, 3.07	120 (sh), 134 (s), 221 (w, br)	zigzag
$Cu(en)_2I_6$[19]	3.376, 2.78	163 (s), 320 (w, br)	zigzag
CsI_3[16]	2.83 (2), 3.03 (2)	93, 102, 137, 148, 157	unsym
$(C_6H_5)_4AsI_3$[16]	2.920 (2)	73, 94, 118	sym
$(TMA{\cdot}H_2O)_{13}HI_5$[20a]	2.74, 3.26	163	linear
$(phenacetin)_2HI_5$[20a]	2.748	119, 185	V shape
$(C_2H_5)_4NI_7$[20a]	2.735, 2.904	183, 115	zigzag
$(PPO)_4I_2$		111 (w), 174 (s)	
$(PPO)_4I_2$		111 (w), 174 (s)	
$(PPO)_{16}I_2$		106 (w), 175 (s)	
$(PPO)_{32}I_2$		111 (w), 168 (s)	
$(PPO)_{64}I_2$		107 (w), 169 (s)	
Et_2O/I_2		206 (vs)	
diglyme/I_2		206 (vs)	

Table I summarizes the Raman data for the $(PPO)_nNaI_x$ system. While the ca. 170-cm^{-1} peak position does not change appreciably as the salt concentration or the iodine loading is increased, the width of this peak increases achieving a maximum for $(PPO)_4NaI_9$ (Table II).

Relatively strong ligands, L, such as pyridine, are known to bring about redox disproportionation of I_2 with the production of polyiodides:

$$mL + nI_2 = I_{2n-1}^- + L_mI^+$$

To test the possibility that a similar disproportionation can be promoted by a weaker ether ligand, the I_2/diglyme and I_2/diethyl ether systems were investigated by Raman spectroscopy. In both instances, only a single peak at 206 cm^{-1} was observed, and this is attributed to free I_2 (see Table III). By contrast the simple polymer iodine complexes (e.g., $(PPO)_8I_2$), which contain no NaI, have Raman spectra that lack any sign of the I_2 modes and display only the polyiodide modes. Apparently the disproportionation reaction (or reaction with trace impurities) is promoted more strongly by the polymer than by diglyme or diethyl ether. Presumably the addition of I_2 to the polymer with or without added salt forms polyiodides by interactions with both existing iodide or polyiodide anions and by disproportionation. The disproportionation reaction seems to dominate when large amounts of iodine are added.

(19) Duker, H.-U.; Freckmann, B.; Niebuhr, H.; Plewa, M.; Tebbe, K.-F. *Z. Kristallogr.* **1979**, *149*, 131.

(20) Kiefer, W.; Bernstein, H. J. *J. Raman Spectrosc.* **1973**, *1*, 417. Teitelbaum, R. C.; Ruby, S. L.; Marks, T. J. *J. Am. Chem. Soc.* **1979**, *101*, 7568. Marks, T. J.; Kalina, D. W. *Highly Conductive Halogenated Low Dimensional Materials in Extended Linear Chain Compounds*; Miller, J. S., Ed.; Plenum: New York, 1982 Vol. 1, pp 197–311. Nour, E. M.; Chen, L. H.; Laane, J. *J. Phys. Chem.* **1986**, *90*, 2841.

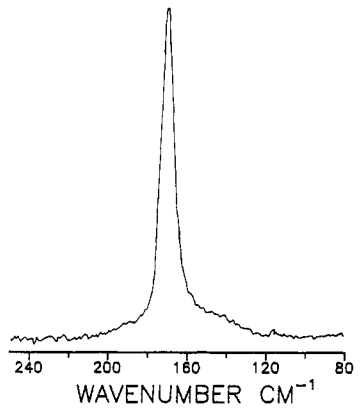

Figure 2. Resonance Raman spectrum of $Cd(NH_3)_4I_6$, one peak due to $(I_3^-)_\infty$ chains at 171 cm^{-1}. ν_0 = 647.1 nm.

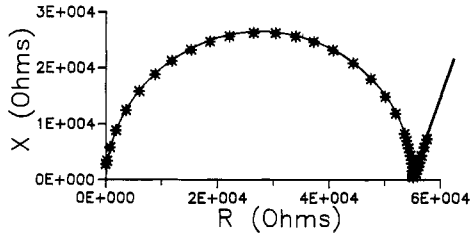

Figure 3. Cole–Cole plot of $(PPO)_4NaI$ at 120 °C.

Raman spectra of crystallographically characterized salts containing polyiodide chains were obtained for comparison with the polymer polyiodide complexes. Figure 2 shows the resonance Raman spectrum of $Cd(NH_3)_4I_6$, which contains nearly straight, infinite chains of $(I^-\cdot I_2)$ with I–I distances of 3.37 and 2.74 Å.[9] The spectrum consists of only one band at 171 cm^{-1} with a peak width at half-height of 7 cm^{-1}. This peak, though narrower than those in $(PPO)_nNaI_x$, correlates well with the 170-cm^{-1} peak observed in the polymer complexes. Raman data for various polyiodide species are summarized in Table III. Compounds containing short isolated polyiodide chains such as I_5^- in $(TMA\cdot H_2O)_{10}HI_5$ (163 cm^{-1}), I_7^- in $(C_2H_5)_4NI_7$ (183, 115 cm^{-1}), or zigzag $(I_3^-)_\infty$ in $Ru(Me_2dtc)_3$ (155 cm^{-1}) show bands at wavenumbers other than 170 cm^{-1}. Since these features are not observed in the polymer iodine complexes, the existence of these types of polyiodides can be ruled out.

Dielectric Response. Simple PPO–NaI complexes and complexes with low iodine loading give nonohmic responses characteristic of ionic conductors. On the other hand, at higher I_2 concentrations, an ohmic response is observed at low frequencies. For example, slow cyclic voltammograms (+20 to −20 mV at 1 mV/s) of these samples give a straight line with a slope matching the bulk resistance value obtained from the low-frequency touchdown of the arc in the ac impedance experiment. Our focus in this study is to explore the underlying processes responsible for the electronic conductivity in systems of the type $(PPO)_nNaI_x$. Figure 3 shows the complex impedance plot for $(PPO)_4NaI$ with ion-blocking electrodes (gold-coated tantalum). This plot has the characteristic shape of an ionic conductor, an arc touching down on the real axis with a low-frequency spur. For polyiodide-containing materials, such as $(PPO)_8NaI_9$, the impedance spectrum consists of the arc alone; the absence of a spur down to the limit of the experiment, 25 mHz, indicates negligible interfacial polarization. All complexes containing polyiodides (indicated by the 170-cm^{-1} Raman band) show no spur. Thus, the cyclic voltammograms and complex impedance data for the polyiodide-containing samples indicate an ohmic electrode–electrolyte interfacial impedance. As described by Lerner et al.[3] a low-frequency second arc is seen for polyiodides in poly[bis((methoxyethoxy)ethoxy)phosphazene] (MEEP), but this feature is attributed to charge transfer of an interfacial process associated with electrode corrosion. In the present work with PPO as the polymer host, a low-frequency arc was not observed with gold electrodes below 50 °C.

Table IV. DSC Data (kelvin) for PPO and Its Complexes[a]

	n				
	4	8	16	32	64
$(PPO)_nNaI_x$					
x = 1	301	282			
x = 3	288	272	251		
x = 5	272	266	245		
x = 7	255	263	243		
x = 9	251	250	245		
$(PPO)_nI_2$		207	207	207	206

[a] For PPO T_g = 206 K.

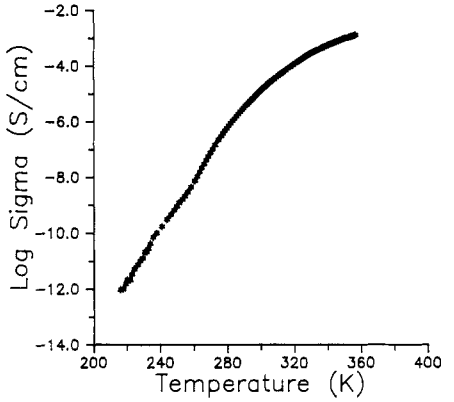

Figure 4. Four-probe data, log σ vs temperature (K), for $(PPO)_8NaI_5$. Point of inflection in the data at T_g.

In polymer salt complexes the ionic conductivity can be described by the Vogel–Tammann–Fulcher (VTF) equation:[4-6]

$$\sigma = AT^{-1/2} \exp\{-B/(T - T_0)\} \quad (1)$$

where T_0 is related to the glass transition temperature, T_g, of the polymer salt complex ($T_0 \approx T_g - 50$). The exponential temperature factor, $T - T_0$ is a function of the degree of local segmental motion within the polymer, which in turn, is responsible for the conduction of ions. Below the glass transition temperature of the polymer salt complex the ionic conductivity ceases due to the loss of local polymer segmental motion. The dependence of the glass transition temperature, T_g, on composition was investigated by using DSC. Table IV shows that the formation of a polymer salt complex increases the T_g from 206 K for neat PPO to about 300 K for $(PPO)_4NaI$. T_g decreases almost linearly with I_2 addition, while addition of I_2 to the polymer itself has no effect on T_g. By contrast, in the case of $(MEEP)_nLiI_x$, the addition of iodine increases T_g.[3] This different response to polyiodide formation is not understood, but since the conductivity increases with I_2 loading in both systems, it appears that polyiodide conductivity is not strongly dependent on the segmental motion of the organic polymer.

The temperature dependence of the four-probe dc conductivity measurements illustrated in Figure 4 provides a more direct probe of the relation between polyiodide conductivity and polymer segmental motion. The striking feature in Figure 4 is the gentle inflection in the conductivity around T_g and the substantial conductivity below

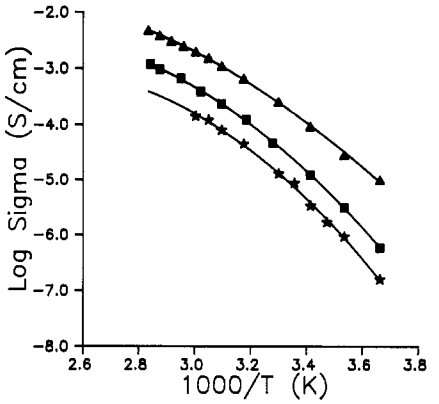

Figure 5. log conductivity vs $1/T$ for (bottom curve) $(PPO)_{16}NaI_5$, (middle curve) $(PPO)_8NaI_5$, and (top curve) $(PPO)_4NaI_5$. The conductivity increases with increasing salt–polyiodide concentration in the polymer.

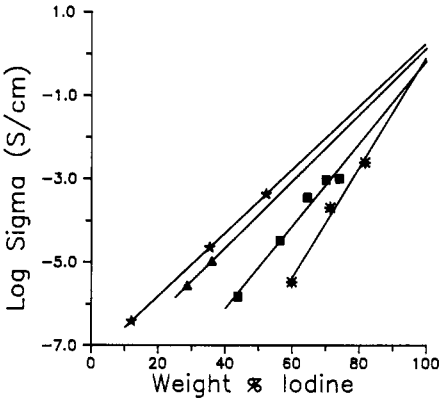

Figure 6. Plot of log conductivity (300 K) vs weight percent iodine for various salt loadings: $(PPO)_nI_2$ (star), $(PPO)_{16}NaI_x$ (triangle), $(PPO)_8NaI_x$ (square), and $(PPO)_4NaI_x$ (starred circle). The data extrapolates to roughly the same conductivity for each salt loading for 100% iodine.

T_g. This temperature dependence, which is characteristic of other samples with high polyiodide content, contrasts sharply with simple ionic conductors, which follow eq 1 and have negligible conductivity below T_g. Unlike simple ion motion, the polyiodide conduction process is only weakly coupled to polymer dynamics. Below T_g, where the polymer segmental motion has ceased, the conductivity data apparently represent the intrinsic conductivity of the polyiodide chains.

The conductivity of polyiodide complexes rises with both increasing salt concentration as shown in Figure 5 and increasing iodine loading at constant salt concentration. The conductivity at 300 K versus percent iodine loading for each salt concentration is plotted in Figure 6. The maximum conductivity for each salt concentration at 300 K for 100% polyiodide can be extrapolated to be approximately 1.15 ± 0.5 S/cm. This extrapolated value is much higher than that observed in either solid iodine ($\sigma = 5 \times 10^{-12}$ S/cm perpendicular to the *bc* plane and 1.7×10^{-8} S/cm within the plane at room temperature)[21] or molten iodine (σ = (0.6–6.0) $\times 10^{-5}$ S/cm at 413 K).[16,22] More information of the compositional effects on the conductivity in related systems has been discussed elsewhere.[3]

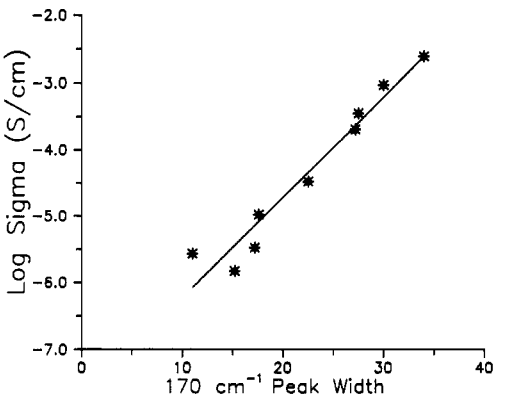

Figure 7. Plot of log conductivity (300 K) vs peak width at half height (170-cm^{-1} peak) for various complexes. The conductivity increases with increasing width of the resonance Raman peak assigned to polyiodides.

A positive correlation was noted between the width of the 170-cm^{-1} polyiodide Raman band and the conductivity of the corresponding samples (Figure 7). The log of the conductivity is plotted against the width of the 170-cm^{-1} peak, which, as stated earlier, appears to be a function of both the number and the length of polyiodide chains. Presently, we do not know whether this correlation is coincidental or intimately connected with the dynamic charge-transport model qualitatively outlined below.

Charge-Transport Mechanism. At high polyiodide concentrations, charge transport is dominated by a process that is much faster than the diffusion of simple ions in polymers. Several models are candidates for the activated charge-transport processes in the polyiodide systems. The most appealing model is based on a Grotthus type ion relay mechanism in which I^- ions are shuttled along or between chains,[16,22] analogous to the conductivity mechanism of protons through aqueous solution.[23] Another possible charge-transport mechanism is a rigid conduction band comprised of iodine valence orbitals in the chain, and finally electron or hole hopping might occur. The hopping mechanism might include simple activated behavior as well as a variable-range hopping (VRH).

The ion relay mechanism has been suggested by a number of authors[16,24,25] to explain observed conductivities in iodine- and polyiodide-containing materials. This mechanism relies on shuttling I^- by rearrangement of long and short bonds along a polyiodide chain, which schematically might be represented as

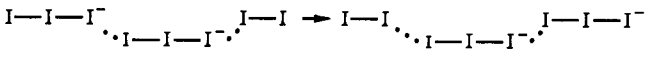

The ion relay mechanism can result in an ohmic response if the iodine–iodide couples are reversible at the electrode electrolyte interface, such as[25]

$$I_3^- + e^- \rightarrow I_3^{2-} \quad \text{at the cathode}$$

$$I_3^{2-} + I_3^- \rightarrow I_2 + I_4^{2-} + e^- \quad \text{at the anode}$$

$$I_4^{2-} \rightarrow I_4^- + e^- \quad \text{at the anode}$$

(21) Greenwood, N. N.; Earnshaw, E. In *Chemistry of the Elements*; Pergamon Press: Oxford, 1984; p 938.
(22) Lewis, G. N.; Wheeler, P. *Z. Phys. Chem.* **1906**, *56*, 179. Rabinowitsch, M.; *Z. Phys. Chem.* **1926**, *119*, 70. Plotnikow, W. A.; Fialkow, J. A.; Tschalij, W. P. *Z. Phys. Chem.* **1935**, *A172*, 307.
(23) Robinson, R. A.; Stokes, R. H. *Electrolyte Solutions*, 2nd ed.; Butterworths: London, 1968.
(24) Bargeman, D.; Kommandeur, J. *Chem. Phys.* **1968**, *49*, 4069. Bejerano, T.; Gileadi, E.; *J. Electroanal. Chem.* **1977**, *82*, 209. Wu, C.; Kim, B.; Kao, H. I.; Rubinstein, I.; Bixon, M.; Gileadi, E. *J. Phys. Chem.* **1980**, *84*, 715. Griffin, C. W.; Jones, M.; Labes, M. M. *Mol. Cryst. Liq. Cryst.* **1982**, *88*, 317.
(25) Alvarez, S.; Novoa, J. *Chem. Phys. Lett.* **1986**, *132*, 531.

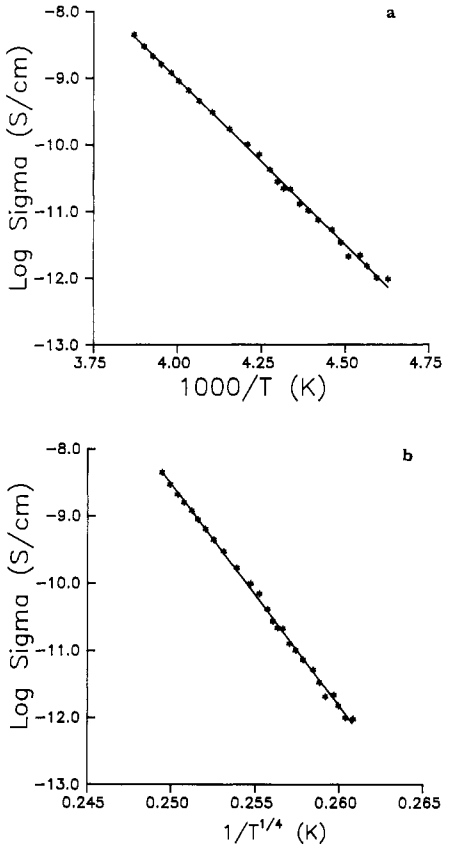

Figure 8. Four-probe data, (a) log conductivity vs $1/T$ (K) and (b) log conductivity vs $1/T^{1/4}$, for $(PPO)_8NaI_5$ below T_g (266 K).

where the bulk charge transfer and incorporation of the products at each electrode into the bulk polyiodide network are faster than the time scale of the measurement.

Electron delocalization has been suggested to occur along polyiodide chains because there are often short contacts between I_3^- or I_5^- species. In several conducting complexes, for instance, the $(benzophenone)_9(KI)_2I_7CHCl_3$ channel complex,[26] the polyiodide chains appear to be the only possible conduction pathway, and semiconductor-like electronic conduction has been proposed to occur along the polyiodide chains. The electronic structure and the role of electron delocalization of long polyiodide chains with high electrical conductivity have been studied theoretically.[27] These compounds are predicted to be semiconductors, and electron delocalization should be most extensive for infinite $(I_3^-)_\infty$ chains. The gap energy is predicted to decrease in the following order: isolated I_2 > isolated I_3^- > infinite chains of $(I_5^-)_\infty$ > infinite chains of $(I_3^-)_\infty$, while bond-length asymmetry has been calculated to greatly increase the bandgap in all cases.[27] The question of charge carrier mobility, which will ultimately determine the observed conductivity in such complexes, was not addressed. Qualitatively a rigid-band model is not appealing because the highly compliant polyiodide network should favor a hopping.

A variable range hopping (VRH) mechanism,[28] with electrons or holes as charge carriers, could also account for the observed ohmic electrical response. In solid I_2, holes have been proposed as charge carriers,[29] while in doped

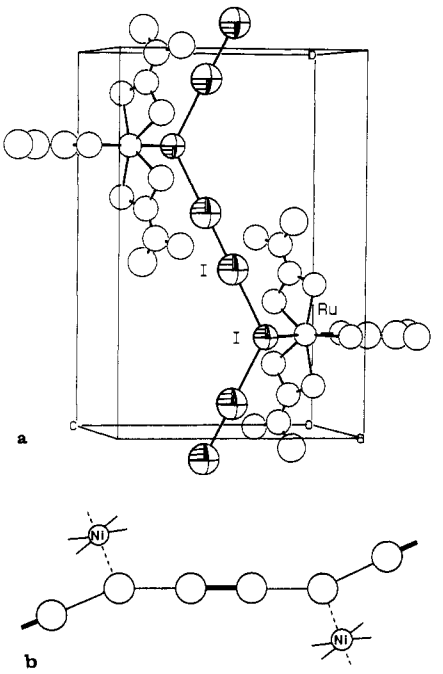

Figure 9. (a) ORTEP view of the $Ru(Me_2dtc)_3I_3$ unit cell;[10] (b) model of $Ni(en)_2I_6$, depicting the nickel coordination to the polyiodide chain.[17]

polyacetylene soliton hopping is used to explain the observed electrical behavior.[30] The VRH mechanism predicts a $T^{-1/n}$ (n = 4) temperature dependence for the conductivity; however, values for n ranging from n = 2 to 4 have been used to fit conductivity data.[31]

The temperature dependence of the conductivity was plotted to determine which, if any, conduction pathways might best describe our systems. The four-probe conductivity data of the polymer-based polyiodides give reasonable fits for n ranging from n = 1 to 4; see Figure 8. Over the temperature range in which we could make measurements, the conductivity data do not allow us to distinguish between competing models.

Some additional insights into the conduction process can be obtained by examining the conductivities of the structurally characterized crystalline polyiodide compounds. The four-probe dc conductivities at 25 °C of $Ni(en)_2I_6$ and $Ru(Me_2dtc)_3I_3$ are 2.8×10^{-10} and $<6 \times 10^{-11}$ S/cm, respectively, and are a stark contrast to the conductivities observed for the polymer–polyiodide complexes. As shown in Figure 9 both of these crystalline compounds contain infinite zigzag chains of I_3^- species with the repeating pattern of bond lengths being long, long, short. The published thermal ellipsoids and the bonding of every third iodine in a chain to a transition metal suggests that an ion relay mechanism is unlikely in these materials. Presumably then only a rigid-band model or hopping mechanism could occur in these polyiodides. Apparently the rigid-band or hopping mechanisms are not efficient processes in the metal complex polyiodides. The VRH or the ion relay mechanism, on the other hand, might be appropriate models for the polymer polyiodides. As with

(26) Perlstein, J. H. *Angew, Chem.* **1977**, *89*, 534.
(27) Kertesz, M.; Vonderviszt, F. *J. Am. Chem. Soc.* **1982**, *104*, 5889.
(28) Mott, N. F. In *Conduction in Non-Crystalline Materials*; Clarendon Press: Oxford, 1987. Mott, N. F.; Davis, E. A. In *Electronic Processes in Non-Crystalline Materials*, 2nd ed.; Clarendon Press: Oxford, 1979.
(29) Siebrand, W. *J. Chem. Phys.* **1964**, *41*, 3574.
(30) Feldblum, A.; Bigelow, R. W.; Gibson, H. W.; Epstein, A. J. *Mol. Cryst. Liq. Cryst.* **1984**, *105*, 191. Epstein, A. J.; Bigelow, R. W.; Feldblum, A.; Gibson, H. W.; Hoffman, D. M.; Tanner, D. B. *Synth. Met.* **1984**, *9*, 155.
(31) Colson, R.; Nagels, P. *J. Non-Cryst. Solids* **1980**, *35–36*, 129. Shacklette, L. W.; Toth, J. E. *Phys. Rev. B* **1985**, *32*, 5892. Park, Y. W.; Lee, Y. S.; Park, C.; Shacklette, L. W.; Baughman, R. H. *Solid State Commun.* **1987**, *63*, 1063.

other authors we favor the ion relay mechanism.[24]

Acknowledgment. This research was supported by DOE through Grants FG02-86ER13640 and DEFG02-89ER45220. Facilities of the NSF-DMR sponsored Northwestern University Materials Research Center were used extensively in this research. We thank Dr. Stephen Harper of Arco Chemicals for samples of PPO. We also thank Dr. Kate Doan, Dr. Michael Lerner, Dr. Leslie Lyons, and Professor Mark Ratner for helpful discussions.

Registry No. PPO, 25322-69-4; NaI, 7681-82-5; I_2, 7553-56-2.

Second Harmonic Generation by the Self-Aggregation of Organic Guests in Molecular Sieve Hosts

Sherman D. Cox,† Thurman E. Gier, and Galen D. Stucky*

Department of Chemistry, University of California at Santa Barbara, Santa Barbara, California 93106

Received March 22, 1990

Inclusion of polar organic molecules in molecular sieve hosts has been investigated as a means of creating self-assembled aggregates of molecules that possess the noncentrosymmetry required for materials to exhibit second harmonic generation (SHG). Aluminophosphate molecular sieves with one-dimensional channel structures are shown by SHG powder measurements to successfully direct this self-aggregation for a number of organic molecules including and related to *p*-nitroaniline. Models supported by FTIR evidence show the aggregates could be chains of molecules with a large net dipole that form within the molecular sieve channels. The polar host crystal then aligns the aggregates to produce a large bulk dipole moment and the observed SHG signal. Three methods for controlling the SHG intensity within a particular host structure have been elucidated: (1) variation of guest concentration, (2) alteration of guest structure, and (3) changing the charge density on the host framework.

Introduction

Nonlinear optical properties are determined by the bulk hyperpolarizability tensor, $\chi^{(n)}$, a quantity that, in the second-order case, $\chi^{(2)}$, is very sensitive to symmetry restrictions.[1] For a material to exhibit second harmonic generation (SHG) it must have a noncentrosymmetric component. This single restriction dominates any search for new materials for SHG applications. In solid-state inorganic chemistry the search is for families of compositional types with acentric crystal structures, the KTP family, for example.[2] In molecular chemistry the effort is to align molecules so that a net bulk dipole results. This has been accomplished in crystals by using a variety of strategies[1,3] including the use of molecular asymmetry, chirality, hydrogen bonding, dipole reduction, changing counterions in organic or organometallic salts,[4] and making use of noncentrosymmetric rarrangements in centrosymmetric organic crystals.[5] Dipole alignment in poled polymer, sol gel,[6] and Langmuir–Blodgett films is receiving considerable attention because of device applications.[1]

Inclusion chemistry can accomplish optimization of molecular alignment by careful size and shape matching of host and guest. The first reports of inclusion chemistry as a method of generating nonlinear optical materials, were in 1984, by Tomaru et al.[7] They showed that *p*-nitroaniline and closely related organic guests exhibited SHG 4 times that of urea in the presence of β-cyclodextrin. Wang and Eaton demonstrated shortly thereafter that this was indeed due to inclusion[8] and expanded the field[9] to other hosts (thiourea, tris(*o*-thymotide), and deoxycholic acid) and organometallic guests, mainly of the arylmetal tricarbonyl type.

This work[10] is the first to use crystalline inorganic hosts with organic guests. Inorganic hosts appropriate for consideration in nonlinear optical applications include the molecular sieves and layered materials. Host materials

†Present address: Pfizer Inc., Specialty Minerals, 9 Highland Ave., Bethlehem, PA 18017.

(1) (a) Williams, D. J. *Angew. Chem., Int. Ed. Engl.* **1984**, *23*, 690–703. (b) Hann, R. A., Bloor, D.; Eds. *Royal Society of Chemistry Special Publication No. 69: Organic Materials for Nonlinear Optics. The Proceedings of a Conference Organized by the Applied Solid State Chemistry Group of the Dalton Division of The Royal Society of Chemistry, Oxford, 29th-30th June, 1988*; Royal Society of Chemistry: London, UK, 1989. (c) Khanarian, G., Ed. *Proc. SPIE—Int. Soc. Opt. Eng., Nonlinear Optical Properties of Organic Materials*; SPIE: Bellingham, WA, 1988; Vol. 971. (d) Heeger, A. J., Orenstein, J., Ulrich, D. R., Eds. *MRS Symp. Proc., Nonlinear Optical Properties of Polymers*; MRS: Pittsburgh, PA, 1988; Vol. 109. (e) Chemla, D. S., Zyss, J.; Eds. *Nonlinear Optical Properties of Organic Molecules and Crystals*; Academic Press: New York, 1987; Vol. 1.

(2) (a) Gier, T. E. U.S. Patent No. 4,231,838, 1980. (b) Bierlein, J. D.; Gier, T. E. U.S. Patent No. 3,949,323, 1976. (c) Gier, T. E. U.S. Patent No. 4,305,778, 1981. (d) Bierlein, J. D.; Ferretti, A.; Brixne, L. H.; Hsu, W. H. *Appl. Phys. Lett.* **1987**, *50*, 1216. (e) Eddy, M. M.; Gier, T. E.; Keder, N. L.; Cox, D. E.; Bierlein, J. D.; Jones, G.; Stucky, G. D. *Inorg. Chem.* **1988**, *27*, 1856–1858. (f) Stucky, G. D.; Phillips, M. L. F.; Gier, T. E. *Chem. Mater.* **1989**, *1*, 492–509.

(3) Meredith, G. R. *M.R.S. Bull.* **1988**, *13*(8), 24–29.

(4) Marder, S. R.; Perry, J. W.; Schaefer, W. P. *Science* **1989**, *245*, 626–628.

(5) Weissbuch, I.; Lahav, M.; Leiserowitz, L.; Meredith, G. R.; Vanherzeele, H. *Chem. Mater.* **1989**, *1*, 114–118.

(6) Zink, J. I.; Kaner, R. B.; Dunn, B., private communication.

(7) (a) Tomaru, S.; Zembutsu, S.; Kawachi, M.; Kobayashi, M. *J. Inclusion Phenom.* **1984**, *2*, 885–890. (b) Tomaru, S.; Zembutsu, S.; Kawachi, M.; Kobayashi, M. *J. Chem. Soc., Chem. Commun.* **1984**, 1207–1208.

(8) Wang, Y.; Eaton, D. F. *Chem. Phys. Lett.* **1985**, *120*, 441–444.

(9) (a) Eaton, D. F.; Anderson, A. G.; Tam, W.; Wang, Y. *J. Am. Chem. Soc.* **1987**, *109*, 1886–1888. (b) Tam, W.; Eaton, D. F.; Calabrese, J. C.; Williams, I. D.; Wang, Y.; Anderson, A. G. *Chem. Mater.* **1989**, *1*, 128–140.

(10) Preliminary results have been published: (a) Cox, S. D.; Gier, T. E.; Stucky, G. D.; Bierlein, J. *J. Am. Chem. Soc.* **1988**, *110*, 2986–2987. (b) Cox, S. D.; Gier, T. E.; Stucky, G. D.; Bierlein, J. *Solid State Ionics* **1989**, *32/33*, 513–520.

0897-4756/90/2802-0609$02.50/0